

# An XMM-Newton view of FeK $\alpha$ in High Mass X-rays Binaries

A. Giménez-García<sup>1</sup>, J. M. Torrejón<sup>1 2</sup>, W. Eikmann<sup>3</sup>, S. Martínez-Núñez<sup>2</sup>, L. M. Oskinova<sup>4</sup>, J. J. Rodes-Roca<sup>1 2</sup>, and G. Bernabéu<sup>1 2</sup>

<sup>1</sup> University Institute of Physics Applied to Sciences and Technologies, University of Alicante, P.O. Box 99, E03080 Alicante, Spain  
e-mail: angelgimenez@ua.es

<sup>2</sup> X-ray Astronomy Group. Departamento de Física, Ingeniería de Sistemas y Teoría de la Señal, University of Alicante, P.O. Box 99, E03080 Alicante, Spain

<sup>3</sup> Dr. Karl Remeis-Sternwarte FAU Erlangen-Nürnberg, D96049 Bamberg, Germany

<sup>4</sup> Institute for Physics and Astronomy, University of Potsdam, D-14476 Potsdam, Germany

## Abstract

We present a comprehensive analysis of the whole sample of available XMM-Newton observations of High Mass X-ray Binaries (HMXBs) until August, 2013, focusing on the FeK $\alpha$  emission line. This line is a key tool to better understand the physical properties of the material surrounding the X-ray source within a few stellar radii (the circumstellar medium). We have collected observations from 46 HMXBs, detecting FeK $\alpha$  in 21 of them. We have used the standard classification of HMXBs to divide the sample in different groups. We find that: (1) FeK $\alpha$  is centred at a mean value of 6.42 keV. Considering the instrumental and fits uncertainties, this value is compatible with ionization states lower than Fe XVIII. (2) The flux of the continuum is well correlated with the flux of the line, as expected. Eclipse observations show that the Fe fluorescence emission comes from an extended region surrounding the X-ray source. (3) FeK $\alpha$  is narrow ( $\sigma_{line} < 0.15$  keV), reflecting that the reprocessing material does not move at high speeds. We attempt to explain the broadness of the line in terms of three possible broadening phenomena: line blending, Compton scattering and Doppler shifts (with velocities of the reprocessing material  $V \sim 1000$  km/s). (4) The equivalent hydrogen column ( $N_H$ ) directly correlates with the EW of FeK $\alpha$ , displaying clear similarities to numerical simulations. It highlights the strong link between the absorbing and the fluorescent matter. The obtained results clearly point to a very important contribution of the donor's wind in the FeK $\alpha$  emission and the absorption when the donor is a supergiant massive star.

## 1 Introduction

Fe lines in the spectral region of  $\sim 6-7$  keV (the Fe complex) have been studied in a large number of X-ray sources given its fruitfulness as a tool for plasma diagnostics. The most recent X-ray space missions (Swift, Suzaku, Chandra and XMM-Newton) have triggered a notable improvement in the attainable spectral resolution and effective area, permitting to distinguish between different emission features in the Fe complex: narrow and broad fluorescence lines (FeK $\alpha$  and FeK $\beta$ ), Compton shoulders and recombination lines (Fe xxv and Fe xxvi) [1]. This improvement has given a remarkable impetus in the study of the Fe complex, and motivates a comprehensive analysis in HMXBs. Fluorescence is produced as a consequence of the X-ray illumination of matter. When an Fe atom absorbs a photon carrying sufficient energy to remove an electron from its K-shell ( $E > 7.2$  keV), the vacancy can be occupied by another electron from an outer shell. If the electron comes from the L-shell, the transition produces FeK $\alpha$  emission. FeK $\beta$  emission is produced when the vacancy is filled by a former M-shell electron. When Fe is more ionized than Fe XIX, the fluorescence yield starts to decrease with the ionization state [3]. Therefore, FeK $\alpha$  is a footprint of not extremely ionized Fe (less than Fe xx). On the other hand, recombination lines Fe xxv and Fe xxvi unveil the presence of very hot gas, where Fe atoms are almost completely stripped. HMXBs are specially susceptible to be studied using the Fe complex, on account of the significance of the circumstellar medium in the observable phenomena. These systems consists of a compact object, either a neutron star (NS) or a black hole (BH), accreting matter from a massive OB star (usually called optical or normal star of the system). In HMXBs the observed luminosity is commonly powered via accretion. Consequently, the way that matter is accreted from the donor directly defines the observable luminosity features of every source.

## 2 Observations and data treatment

Summarizing the sample of observations, we have collected data from 46 HMXBs. 21 of them exhibit FeK $\alpha$  emission. We note that some sources have more than one available observation. Taking everything into account (46 sources, temporal splitting depending on the state of the source, and more than one observation per source in some cases), we end up with a total number of 108 spectra that we have analysed. We have followed the catalogue of [2], in addition to later discoveries or confirmations, to identify the currently known HMXBs, and used every available XMM-Newton public observation<sup>1</sup>. The sources not included in the Liu catalogue, but here considered, are: HD 119682, SS 397, IGR J16328-4726, HD 45314, HD 157832, Swift J045106.8-694803, IGR J16207-5129 and XTE J1743-363.

---

<sup>1</sup><http://xmm.esac.esa.int/xsa/>

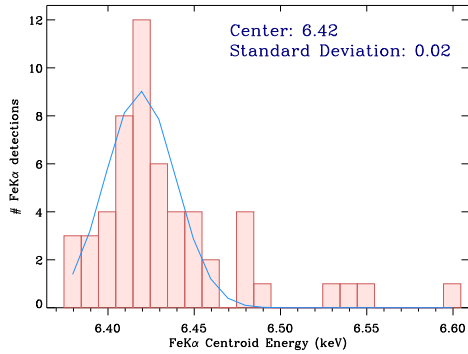


Figure 1: Centroid energy of  $FeK\alpha$ , with a Gaussian fit overplotted (blue profile). The mean value is  $6.42 \pm 0.02$  keV, compatible with Fe I-XVIII.

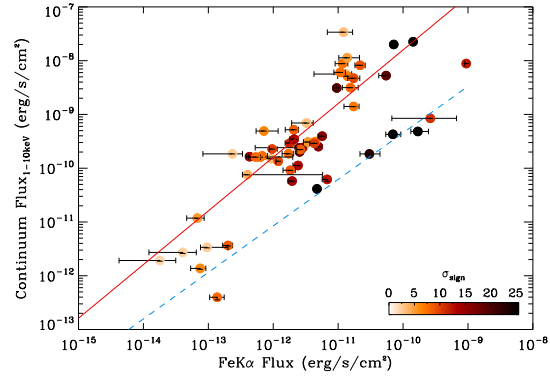


Figure 2:  $F_{1-10keV}$  versus  $F_{FeK\alpha}$ . Blue dashed line marks the correlation observed for IGR J16318-4848 jointly with eclipse observations, and the red solid line follow the bulk of the observations. The color map indicates the statistical significance of the line.

## 3 Results

### 3.1 Centroid energy

In Figure 1 we can see an histogram presenting the centroid energy of  $FeK\alpha$ . A Gaussian fit of the data reveals a mean value for the centroid energy of 6.42 keV. The standard deviation is 0.02 keV, comparable to the the error that we typically obtain in the estimation of the centroid energy in the fits. Taking into account the standard deviation and the uncertainties in the CTI corrections in EPN<sup>2</sup>, the centroid energy of  $FeK\alpha$  constrains the ionization state of Fe to less ionized than Fe XVIII [3], in agreement with previous studies in HMXBs [1, 4, 5]. In this regard, the study of [1] using HETGS (more accurate in wavelength than EPN), gives a narrower constrain in the ionization state (Fe I-X). Our present work support this result adding more sources to the sample. In the right side of Figure 1 we can see seven  $FeK\alpha$  detections emerging out of the Gaussian profile. Four of them are unlikely to be described by such a Gaussian profile, since they lie more than three times the standard deviation away from the mean energy. All four belong to Cygnus X-1.

#### 3.1.1 Continuum Flux vs $FeK\alpha$ Flux

In Figure 2 we have represented the unabsorbed flux of the continuum between 1-10 keV cancelling  $FeK\alpha$  emission ( $F_{1-10keV}$ ), against the flux of  $FeK\alpha$  ( $F_{FeK\alpha}$ ). In a logarithmic scale, we identify two different patterns of correlation. First, for a subset including all the

<sup>2</sup>Please find more information about long-term CTI correction in the release note *EPIC-pn Long-Term CTI*, by M.J.S Smith et al. (2014), at <http://xmm2.esac.esa.int/docs/documents/CAL-SRN-0309-1-0.ps.gz>; and *EPIC status of calibration and data analysis* by Guainazzi (2008), at [http://xmm2.esac.esa.int/external/xmm\\_sw\\_cal/calib/CAL-TN-0018.ps](http://xmm2.esac.esa.int/external/xmm_sw_cal/calib/CAL-TN-0018.ps).

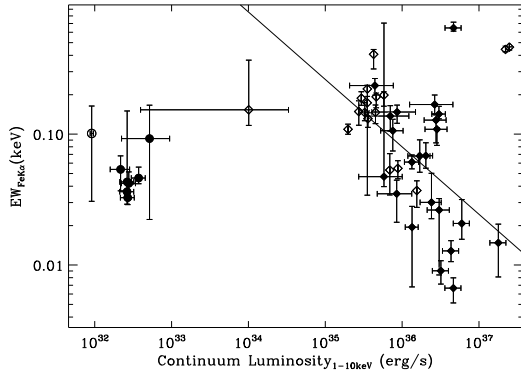


Figure 3: EW of FeK $\alpha$  against  $L_{1-10\text{ keV}}$ .  $\gamma$  Cassiopeae analogs (circles) lie at  $L_{1-10\text{ keV}} < 10^{33}$  erg/s. Open symbols indicate that either the distance either the error in the estimation of the distance is unknown. The solid line corresponds to a linear fit in logarithmic scale of the filled diamonds, that is, the sources with available distance with error estimation and  $L_{1-10\text{ keV}} > 10^{33}$  erg/s.

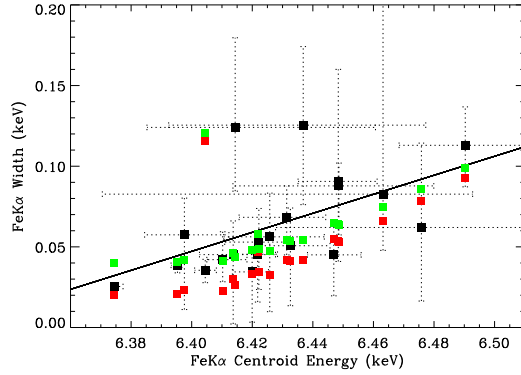


Figure 4: Width of FeK $\alpha$  ( $\sigma_{line}$ ) versus the centroid energy (black squares). Black solid line traces a linear fit. We have marked in colour the expected width from the contribution of three different broadening phenomena: line blending, Compton broadening and Doppler shifts, considering velocities of  $V(\text{km/s}) = 1000$  (red) and  $V(\text{km/s}) = 2000$  (green).

eclipse observations and IGR J16318-4848, we find a correlation with Pearson Coefficient (PC) of 0.98 (blue dashed line). Second, for the rest of observations, we find a correlation with PC=0.89 (red solid line). The observed divergence among eclipse (plus IGR J16318-4848) and out-of-eclipse observations suggests that the companion star blocks in a different proportion the continuum and the FeK $\alpha$  emission. Therefore, an important contribution of the fluorescence emission is produced in an extended region of  $R > R_*$ . This is consistent with previous analysis of eclipse observations of HMXBs (e.g. [6] and [7]). In particular, [7] estimates that 20% of FeK $\alpha$  in OAO 1657-415 is emitted from 19 light-seconds off the X-ray source. We have also faced the luminosity of the continuum with the EW of FeK $\alpha$ . We have excluded eclipse and IGR J16318-4848 from this analysis, given that the EW is strongly affected by the high obscuration of the continuum that they suffer from. In Figure 3 we plot the EW of FeK $\alpha$  against the unabsorbed luminosity of the continuum between 1-10 keV cancelling FeK $\alpha$  emission ( $L_{1-10\text{ keV}}$ ). We observe two different groups of sources: 1)  $\gamma$  Cassiopeae analogs lie at low luminosities ( $L_{1-10\text{ keV}} < 10^{33}$  erg/s); 2) the rest of sources which exhibit FeK $\alpha$ .  $\gamma$  Cassiopeae analogs don't show any evident correlation (they are very few points), while the rest present a moderate inverse correlation (PC=-0.25, and PC=-0.39 using only the sources with an available estimation of distance with error, marked as filled diamonds in Figure 3). [8] observed an inverse correlation in the EW of CIV and the UV luminosity in AGNs. Analogously, the decrease of the EW of FeK $\alpha$  when increasing the X-ray luminosity is called *X-rays Baldwin effect*.

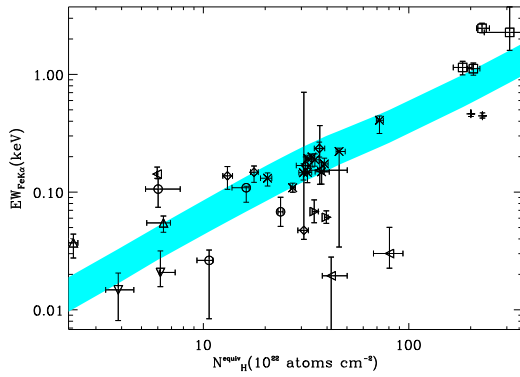


Figure 5: Curve of growth observed for FeK $\alpha$ , that is, EW against  $N_H$ . The turquoise band marks the expected correlation using numerical simulations. The sources are identified by different symbols when more than one observation is included: 4U 1700-37 (open circle), 4U 1907+09 (open upward triangle), Cygnus X-1 (open downward triangle), EXO1722-363 (open diamond), IGR J16318-4848 (open square) and IGR J16320-4751 (plus). Only one observation for Centaurus X-3, GX 301-2, Vela X-1 and XTE J0421+560 (all four a star symbol).

### 3.1.2 FeK $\alpha$ Width vs Centroid Energy

In Figure 4 we present the centroid energy of this feature versus its width ( $\sigma_{line}$ ). We can see a moderate correlation (black line in Figure 4, PC=0.55), indicating a possible blending of lines. Two observations (uppermost side of Fig. 4) do not follow the correlation. They correspond to observations of 4U 1700-37 (Obs.ID 0083280201) and EXO 1722-363 (Obs.ID 0405640201) where the Fe complex is hardly resolved, and therefore it is very likely that a contribution of Fe XXV and Fe XXVI in the model of FeK $\alpha$  is increasing the measured width of the FeK $\alpha$  line. Coloured squares correspond to the expected width from the contribution of three different broadening phenomena: line blending, Doppler shifts and Compton broadening.

### 3.1.3 Curve of growth

In Figure 5 we show, for out of eclipse observations, the  $N_H$  versus the EW of FeK $\alpha$  (what is generally known as the *curve of growth*). We want to take into account observations where  $N_H$  reflects the intrinsic absorption of the system. Hence, we have set  $N_H > 2$  as a condition to safely exceed the typical  $N_H$  of the interstellar medium for the sources here studied (checked using the online application following [9]). The use of this criterion excludes the BeXB SAX J2103.5+4545, the  $\gamma$  Cassiopeae analogs:  $\gamma$  Cassiopeae and HD 110432; and the SFXT IGR J11215-5952. Moreover, eclipse observations show higher EW and they are not comparable to out-of-eclipse observations. Therefore, eclipse observations have not been

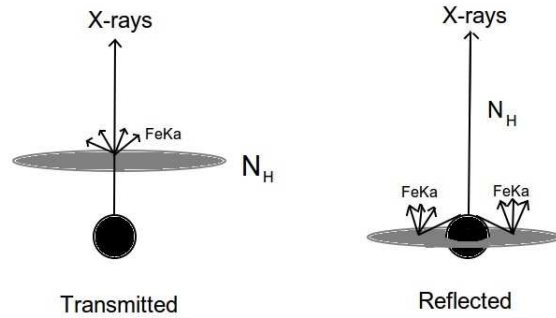


Figure 6: Simple sketch of two plausible configurations of circumstellar matter in HMXBs. In the left side, X-rays are transmitted through a dense medium (e.g. the strong wind of the donor), producing high  $N_H$  directly correlated with the EW of FeK $\alpha$ . In the right side, X-rays are reflected in an accretion disk producing fluorescence, and also transmitted through a more diffuse medium. In this case  $N_H$  is not necessarily correlated with the EW of FeK $\alpha$ .

plotted in Figure 5. As a consequence of the chosen criteria, we end up with a set of 36 observations, where all the donors are supergiants.  $N_H$  and the EW of FeK $\alpha$  are expected to correlate in HMXBs, as shown by [1], since the spectral lines are usually stronger when the optical depth increases. Our sample confirms these expectations, showing a notable correlation (PC=0.85). This correlation highlights that the X-ray absorption is strongly linked to the matter that emits FeK $\alpha$ , being produced by matter in the line of sight, where the X-rays are absorbed, and not in other plausible regions such as an accretion disk. (see a sketch in Figure 6). Namely, in the systems included in Figure 5 (all with a supergiant optical star), FeK $\alpha$  is produced from the transmission of X-rays through the circumstellar medium, that is, either through the strong wind of the supergiant donor either through any structure in the line of sight such as ionization or accretion wakes. We have determined the theoretical curve of growth using numerical simulations. In this simulations there is an input of X-ray radiation with a power law profile, that is transmitted through a cloud of spherically distributed neutral matter [10].

## Acknowledgments

Based on observations obtained with XMM-Newton, an ESA science mission with instruments and contributions directly funded by ESA member states and the USA (NASA). This research has made use of software obtained from NASA's High Energy Astrophysics Science Archive Research Center (HEASARC). The work of AGG has been supported by the Spanish MICINN under FPI Fellowship BES-2011-050874 associated to the project AYA2010-15431.

## References

- [1] Torrejón, J. M. and Schulz, N. S. and Nowak, M. A. and Kallman, T. R. 2010, ApJ, 715, 947
- [2] Liu, Q. Z. and van Paradijs, J. and van den Heuvel, E. P. J. 2006, A&A
- [3] Kallman, T. R. and Palmeri, P. and Bautista, M. A. and Mendoza, C. and Krolik, J. H. 2004, arXiv:astro-ph/0405210, 155, 675
- [4] Gottwald, M. and Parmar, A. N. and Reynolds, A. P. and White, N. E. and Peacock, A. and Taylor, B. G. 1995, A&AS, 109, 9
- [5] Nagase, F. 1989, PASJ, 41, 1
- [6] Rodes-Roca, J. J. and Page, K. L. and Torrejón, J. M. and Osborne, J. P. and Bernabéu, G. 2011, A&A, 526, A64
- [7] Audley, M. D. and Nagase, F. and Mitsuda, K. and Angelini, L. and Kelley, R. L. 2006, MNRAS, 367, 1147
- [8] Baldwin, J. A. 1977, ApJ, 214, 679
- [9] Willingale, R. and Starling, R. L. C. and Beardmore, A. P. and Tanvir, N. R. and O'Brien, P. T. 2013, MNRAS, 431, 394
- [10] Eikmann, W. 2012, Masters Thesis, Dr. Karl Remeis Observatory Bamberg, Astronomical Institute of the Friedrich-Alexander-University of Erlangen-Nrnberg